Energy Geotechnics – Wuttke, Bauer & Sánchez (Eds)
© 2016 Taylor & Francis Group, London, ISBN 978-1-138-03299-6

Temperature distribution in the vicinity of a borehole heat exchanger for intermittent heat extraction: An analytical solution

S. Erol & B. François
Building, Architecture and Town Planning Department (BATir), Université Libre de Bruxelles, Brussels, Belgium

ABSTRACT: Existing analytical solutions for thermal analysis of closed-loop ground heat exchangers systems evaluate temperature change in the heat carrier-fluid and the surrounding ground in the production period of Borehole Heat Exchangers (BHE) only if a continuous heat load is assigned. In the present study, we solve analytically the heat conduction/advection/dispersion equation in porous media, for intermittent heat extraction. We convolute rectangular function or pulses in time domain both for single and multi-BHEs field. The solution includes non-symmetric configurations around the BHEs by considering anisotropic features induced by groundwater convection or intrinsic anisotropy of thermal conductivity. Thermal dispersivity linked to the ground water flow is also considered.

The validity of the analytical model is checked through the comparison with results obtained from numerical finite element code. The comparison results agree well with numerical results both for conduction and advection dominated heat transfer systems, and analytical solutions provide significantly shorter runtime compared to numerical simulations. The developed tool allows also to investigate the recovery aspects and the sustainability of closed-loop ground heat exchangers systems in terms of temperature and the energy deficit of the ground.

1 INTRODUCTION

The Ground Source Heat Pump (GSHP) system technologies are the most often application of the shallow geothermal energy use and primarily reduce the energy consumption for the space heating and cooling supplied from the conventional systems.

In order to evaluate the necessary drilling depth of a borehole heat exchanger and the regulation of the heat input, the specific heat extraction rate should be optimized regarding the characteristics of the hydrogeological conditions for the long term operational effects in the fields.

This is particularly the case for multi-BHEs that may affect significantly the ground temperature on a relatively large area. After an operation period of BHEs, the ground needs time to recover from the temperature drop to sustain the performance of the system in the long-term run (e.g. 30 years) (Signorelli 2004; Rybach and Eugster 2010).

In order to investigate an operation both with the heat extraction and the subsequent recovery periods of BHEs, including the groundwater flow dispersion in a porous medium and the axisymmetric heat transfer along the BHE, the 3D numerical simulation tools undergo a large computational effort and require long execution time. On the other hand, most of the analytical solutions described in literature consider a constant continuous heat extraction/injection in time merely for a single BHE (Eskilson 1987; Zeng et al. 2002; Sutton et al. 2003; Diao et al. 2004; Marcotte et al. 2010; Man et al. 2010; Molina et al. 2011). Until now, intermittent heat extraction can be taken into account through simplified assumptions (Eskilson 1987; Hellström 1991; Claesson and Eskilson 1988).

The objective of this study is to develop an analytical solution to evaluate temperature change in the ground both for single and multi-BHEs that considers intermittent heat extraction, thermal conduction, advection and dispersion. This new analytical solution may further help to investigate the regulatory issues such as the recovery of groundwater temperature after the use of GSHP systems, and also can be used in TRT operations for predicting the ground thermal properties (Erol et al., 2015).

We start from the Green's function which is the solution of heat conduction/advection/dispersion equation in porous media and apply an analytical convolution of that function with a rectangular function or pulses, which have different period length and pulse height. The evolution of the mean fluid temperature of the carrying fluid to maintain a constant heat extraction rate is evaluated along the time. Temperature evaluation in the surrounding ground is also deduced. The developed equation is verified with the finite element method software COMSOL Multiphysics. Furthermore, the energy balance of the ground is investigated with the analytical solution during 30 years of production period, and the subsequent energy recovery of the ground after the system is shutdown.

2 ANALYTICAL DEVELOPMENT

2.1 *Single BHE*

In geothermal literature, the existing finite and cylindrical analytical solutions with a constant heat load may provide satisfactory estimation of ground thermal parameters to design closed-loop ground heat exchangers systems (Deerman and Kavanaugh 1991; Kavanaugh and Rafferty 2014; Gehlin 2002). In a real case, the systems can be operated with various periods in a given time for different heat extraction/injection rates, instead of a continuous operation as assumed in most of other previously presented analytical methods. Some authors evaluated the temperature change for TRT operation in the vicinity of a single BHE or BHEs field with an analytical solution by using multiple load aggregation algorithms (Yavuzturk 1999; Bernier et al. 2004; Marcotte and Pasquier 2008; Lamarche 2009; Michopoulos and Kyriakis 2009; Michopoulos and Kyriakis 2010). However, some of those approaches may not be appropriate in all cases to evaluate the accurate temperature change in the ground due to neglecting the axial effect, considering only single BHE or not taking into account groundwater flow. In particular when Darcy's velocity in porous media is considered, the thermal dispersion coefficients must be taken into account, because thermal dispersion has a large impact on the distribution of the temperature plume around BHE, for Darcy's velocity larger than $\times 10^{-8}$ m/s (Molina et al. 2011).

The governing equation of the heat advection/dispersion in porous media is given as follows:

$$\rho_m c_m \frac{\partial T}{\partial t} = \left(\lambda_x \frac{\partial^2 T}{\partial x^2} + \lambda_y \frac{\partial^2 T}{\partial y^2} + \lambda_z \frac{\partial^2 T}{\partial z^2} \right) - \mathrm{u}_{w,x} \rho_w c_w \frac{\partial T}{\partial x} + s \tag{1}$$

in which $\mathrm{u}_{w,x}$ is the Darcy's velocity on the x-direction, s is a volumetric heat source, and $\rho_m c_m$ is the volumetric heat capacity of the medium, which can be calculated as the weighted arithmetic mean of the solids $\rho_s c_s$ and volumetric heat capacity of water $\rho_w c_w$ (de Marsily 1986):

$$\rho_m c_m = (1-n) \rho_s c_s + n \rho_w c_w \tag{2}$$

The components of effective longitudinal and transverse thermal conductivities are defined on the directions of x, y and z as follows (Hopmans et al. 2002):

$$\lambda_x = \lambda_m + \varpi_l \rho_w c_w \mathrm{u}_{w,x} \tag{3}$$

$$\lambda_y = \lambda_z = \lambda_m + \varpi_t \rho_w c_w \mathrm{u}_{w,x} \tag{4}$$

where λ_m is the bulk thermal conductivity of porous medium in the absence of groundwater flow, ϖ_l and ϖ_t are the longitudinal and transverse dispersivities, respectively. The thermal dispersion is a linear function of groundwater flow and relates to the anisotropy of the velocity field (Molina et al. 2011; Sauty et al. 1982).

The solution of the partial differential equation for heat transfer in porous media (Eq. 1) is obtained from the Green's function G of a pulse point source Q_P at the given point coordinates (x', y', z') and time $t = 0$ (Metzger 2002):

$$\Delta T(x,y,z,t) = \frac{G(x,y,z,t)}{\rho_m c_m} = \frac{Q_P}{8 \rho_m c_m \sqrt{\lambda_x \lambda_y \lambda_z} \left(\frac{\pi t}{\rho_m c_m} \right)^{3/2}} \times \exp\left[-\frac{(x-x')^2}{\frac{4\lambda_x t}{\rho_m c_m}} - \frac{(y-y')^2}{\frac{4\lambda_y t}{\rho_m c_m}} - \frac{(z-z')^2}{\frac{4\lambda_z t}{\rho_m c_m}} \right] \tag{5}$$

In order to take into account the axial effect and the groundwater flow, this solution can be applied for the response of a constant line-source with finite length H along the vertical z direction with a pulse heat extraction after applying moving source theory (Carslaw and Jaeger 1959) by integrating Eq. 5 along the z-axis (Diao et al. 2004):

$$\Delta T(x,y,z,t) = \frac{Q_L}{8 \rho_m c_m \sqrt{\lambda_x \lambda_y \lambda_z} \left(\frac{\pi t}{\rho_m c_m} \right)^{3/2}} \times \int_0^H \exp\left[-\frac{(x-v_T t)^2}{\frac{4\lambda_x t}{\rho_m c_m}} - \frac{y^2}{\frac{4\lambda_y t}{\rho_m c_m}} - \frac{(z-z')^2}{\frac{4\lambda_z t}{\rho_m c_m}} \right] dz' \tag{6}$$

where Q_L is a pulse heat input per meter depth and v_T is thermal transport velocity that can be calculated as follows (Molina et al. 2011):

$$\mathrm{v_T} = \mathrm{u}_{w,x} \frac{\rho_w c_w}{\rho_m c_m} \tag{7}$$

In order to simplify Eq. 6, the exponential function can be integrated by using u-substitution method:

$$\Delta T(x,y,z,t) = \frac{Q_L}{8 \rho_m c_m \sqrt{\lambda_x \lambda_y \lambda_z} \left(\frac{\pi t}{\rho_m c_m} \right)^{3/2}} \times \exp\left[-\frac{(x-v_T t)^2}{\frac{4\lambda_x t}{\rho_m c_m}} - \frac{y^2}{\frac{4\lambda_y t}{\rho_m c_m}} \right] \int_0^H \exp\left[-\frac{(z-z')^2}{\frac{4\lambda_z t}{\rho_m c_m}} \right] dz' \tag{8}$$

$$u^2 = \frac{(z-z')^2}{\frac{4\lambda_z t}{\rho_m c_m}} \rightarrow u = \frac{z-z'}{\sqrt{\frac{4\lambda_z t}{\rho_m c_m}}} \tag{9}$$

$$-\sqrt{\frac{4\lambda_z t}{\rho_m c_m}} du = dz' \tag{8}$$

The limits of u-value becomes:

$$u:\frac{z-H}{\sqrt{\frac{4\lambda_z t}{\rho_m c_m}}}\rightarrow\frac{z}{\sqrt{\frac{4\lambda_z t}{\rho_m c_m}}} \tag{9}$$

Substituting Eq. 10 and Eq. 11 into Eq. 8, allows to re-write the equation as:

$$\Delta T(x,y,z,t)=\frac{Q_L}{8\rho_m c_m\sqrt{\lambda_x\lambda_y\lambda_z}\left(\frac{\pi t}{\rho_m c_m}\right)^{3/2}}\times\exp\left[-\frac{(x-v_T t)^2}{\frac{4\lambda_x t}{\rho_m c_m}}-\frac{y^2}{\frac{4\lambda_y t}{\rho_m c_m}}\right]\int_{\frac{z-H}{\sqrt{\frac{4\lambda_z t}{\rho_m c_m}}}}^{\frac{z}{\sqrt{\frac{4\lambda_z t}{\rho_m c_m}}}}\exp\left(-u^2\right)\left(\sqrt{\frac{4\lambda_z t}{\rho_m c_m}}\right)du \tag{10}$$

The integration of exponential function $f=\exp(-u^2)$ can be expressed with error function:

$$erf(x)=\frac{2}{\sqrt{\pi}}\int_0^x\exp\left(-u^2\right)du\rightarrow\frac{\sqrt{\pi}}{2}erf(x)=\int_0^x\exp\left(-u^2\right)du \tag{11}$$

By taking the integration of exponential function, therefore, Eq. 12 reduces to:

$$\Delta T(x,y,z,t)=\frac{Q_L}{8\rho_m c_m\sqrt{\lambda_x\lambda_y\lambda_z}\left(\frac{\pi t}{\rho_m c_m}\right)^{3/2}}\times\sqrt{\frac{4\lambda_z t}{\rho_m c_m}}\frac{\sqrt{\pi}}{2}\exp\left[-\frac{(x-v_T t)^2}{\frac{4\lambda_x t}{\rho_m c_m}}-\frac{y^2}{\frac{4\lambda_y t}{\rho_m c_m}}\right]\times\left[erf\left(\frac{z}{\sqrt{\frac{4\lambda_z t}{\rho_m c_m}}}\right)-erf\left(\frac{z-H}{\sqrt{\frac{4\lambda_z t}{\rho_m c_m}}}\right)\right] \tag{12}$$

with simplification, Eq. 14 can be expressed with the error functions as follows:

$$\Delta T(x,y,z,t)=Q_L\times\underbrace{\left\{\begin{array}{l}\frac{1}{8\pi t\sqrt{\lambda_x\lambda_y}}\exp\left[-\frac{(x-v_T t)^2}{\frac{4\lambda_x t}{\rho_m c_m}}-\frac{y^2}{\frac{4\lambda_y t}{\rho_m c_m}}\right]\\ \left[erf\left(\frac{z}{\sqrt{\frac{4\lambda_z t}{\rho_m c_m}}}\right)-erf\left(\frac{z-H}{\sqrt{\frac{4\lambda_z t}{\rho_m c_m}}}\right)\right]\end{array}\right\}}_{f(x,y,z,t)} \tag{13}$$

To apply an intermittent injection or extraction of heat in time domain, we convolute analytically Eq. 15 with a single or a series of different rectangular pulses referring to the duration of operations in time. For instance, $f\ (x,\ y,\ z,\ t)$ function is convoluted with a rectangular heat flow rate function $q_L(t)$ defined as follows:

$$q_L(t)=\begin{cases}q_L & \text{for } t\in[0,\mathbf{T}]\\ 0 & \text{otherwise}\end{cases} \tag{14}$$

in which $\mathbf{T}$ is the period of heat extraction. q_L is the heat flow rate taken as independent of the depth in our simulations.

The convolution of q_L and f function is written as follows:

$$\begin{aligned}\Delta T(x,y,z,t)&=\int_{-\infty}^{\infty}q_L(\tau)f(x,y,z,t-\tau)d\tau\\&=q_L\int_0^{\mathbf{T}}f(x,y,z,t-\tau)d\tau\end{aligned} \tag{15}$$

For the analytical evaluation of the convolution integral equation, we discretize both q_L and f functions with a differential of Δt. So, the convolution as a sum of impulse responses at coordinates (x,y,z) is given as:

$$\Delta T(x,y,z,t)=\sum_{i=0}^{n-1}q_L(i\Delta t)f(x,y,z,t-i\Delta t)\Delta t \tag{16}$$

where n denote the time span, $i\ \Delta t$ is the time delay of each unit impulse, and the delayed and shifted impulse response becomes $q_L\ (i\ \Delta t)f(t\text{-}i\ \Delta t)\ \Delta t$.

By using the same method, it is possible to convolute f function with rectangular pulses which have different pulse height and length in given identical time span of f function. Thus, recovery period of the ground can be investigated after a production of a single BHE and the numerical computational effort will be decreased.

2.2 *Multi-BHEs*

In case of multi-BHEs, analytical solution Eq. 15 can be solved in a sum function (Eq. 19) depending on the grid coordinates of each line heat source as illustrated in Figure 1.

$$\Delta T(x,y,z,t)=Q_L\times\sum_{j=1}^{s}\left\{\begin{array}{l}\frac{1}{8\pi\sqrt{\lambda_x\lambda_y}}\frac{1}{t}\\ \times\exp\left\{-\left[\frac{(x-x_j-v_T t)^2}{\frac{4\lambda_x t}{\rho_m c_m}}+\frac{(y-y_j)^2}{\frac{4\lambda_y t}{\rho_m c_m}}\right]\right\}\\ \times\left[erf\left(\frac{z}{\sqrt{\frac{4\lambda_z t}{\rho_m c_m}}}\right)-erf\left(\frac{z-H}{\sqrt{\frac{4\lambda_z t}{\rho_m c_m}}}\right)\right]\end{array}\right\} \tag{19}$$

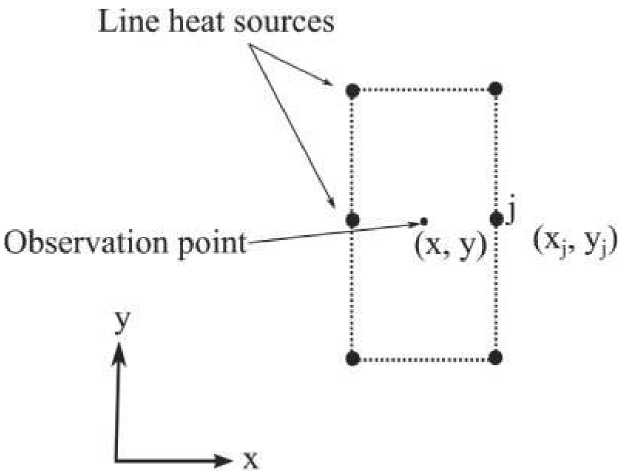

Figure 1. Illustration of multi-BHEs geometry demonstrating the grid coordinates.

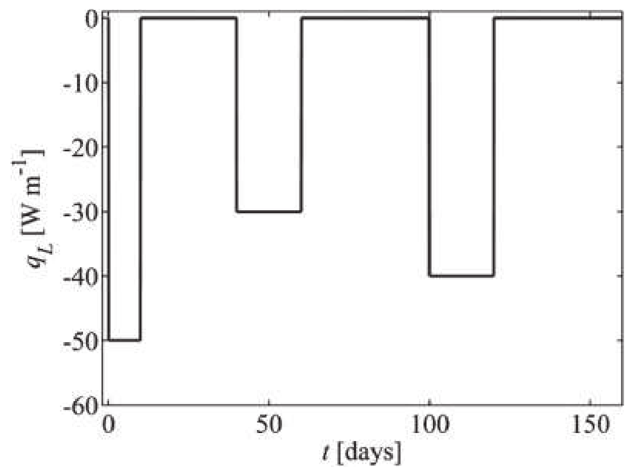

Figure 2. Load profile of heat extraction.

in which s represents the number of BHEs. We consider the impact of groundwater flow on each BHE at x direction by taking into account thermal transport velocity v_T.

The sum $C(x, y, z, t)$ can be convoluted as described in the previous Section 2.1 to apply intermittent heat extraction as follows:

$$\Delta T(x,y,z,t) = \sum_{i}^{n-1} q_L(i\Delta t)C(x,y,z,t-i\Delta t)\Delta t \qquad (17)$$

3 VALIDATION

The developed analytical solutions (Eq. 18 and Eq. 20), for intermittent heat extraction, are verified with 3D numerical models. For the verification, numerical model setup, initial and boundary conditions of the model, input parameters and comparison of the numerical and the analytical solution results are presented in the following.

Table 1. Common initial input parameters for the model domain of single and multi-BHEs field.

Parameters	Value
Initial temperature °C (T_o)	0
Bulk thermal conductivity of porous medium W m^{-1} K^{-1} (λ_m)	2.4[a]
Effective thermal conductivity in the longitudinal direction W m^{-1} K^{-1} (λ_x)	6.6[b]
Effective thermal conductivity in the transverse direction W m^{-1} K^{-1} ($\lambda_y = \lambda_z$)	2.82[b]
Volumetric heat capacity MJ m^{-3} K^{-1} ($\rho_m c_m$)	2.8[a]
Groundwater flow / discharge m s^{-1} ($u_{w,x}$)	1×10^{-6}[c]
Longitudinal thermal dispersion coefficient (ϖ_l)	1[d]
Transverse thermal dispersion coefficient (ϖ_t)	0.1[d]

[a] Representative values taken from (VDI-Richtlinie 2000).
[b] Calculated values according to Eq. 3 and 4.
[c] Assigned only for the models in which heat advection/dispersion is considered.
[d] Values taken from (Hecht-Méndez et al. 2013) to calculate effective thermal conductivities.

3.1 *Numerical model setup*

In order to validate the analytical solution developed above, simple cases for single and multi-BHEs have been considered through numerical models using COMSOL Multiphysics software. The common numerical characteristics are described here for both single and multi-BHEs field models. The study is carried out by a 3D homogeneous model domain and BHE is represented with the line heat source(s) (W m^{-1}). A model domain of 40 m × 40 m in the horizontal direction and 60 m in the vertical direction is set for the simulation. The length of line heat source is 50 m for each. The mesh is generated using uniform tetrahedral elements. The coordinates of single and multi-lines heat sources are shown in Figure 3.

In order to get a better resolution of the temperature variations around the line source, close to it the mesh is further refined along the length of line source and also along the line on which the observation point are placed (at the depth of 25 m).

As the boundary conditions, the load profile of heat extraction with three different extraction periods can be seen in Figure 2. The simulation time is restricted to 160 days. The top of the model surface temperature is fixed to 0°C, as well as identically assigned initial temperature, to observe the relative temperature change in the subsurface. Initial input parameters are given in Table 1. Thermal dispersion is taken into account leading to anisotropic thermal conductivity of the medium, as described by Eq. 3 and 4.

The number of elements changes depending on the model of single or multi-lines heat sources (Table 2). For the simulations, the basic heat transfer module of COMSOL Multiphysics, which uses Fourier's law, is used, and the groundwater flow is imposed through a homogeneous velocity field. The Backward Euler (Crank-Nicolson Scheme) time marching method with RMS error tolerance of 10^{-3} is applied and the maximum time step interval set to 86400 s due to better

Table 2. Summary of the model setup for verification.

Parameter	Value
Type of problem	3D
Numerical method for heat transfer	Standard Galerkin-FEM
Simulation time	160 days
Number of elements solved for single BHE model/multi-BHEs model	834,679/1,975,633
Solver type	Flexible Generalized Minimal Residual method

Table 3. Comparison the execution times and time steps for single BHE.

Model	Number of time step[a] (Total simulation)	Runtime [s] [a]
Analytical solution (Eq. 18)	2562	9[b]/13[c]
Numerical model 1 no groundwater flow	162	15986
Numerical model 2 with groundwater flow of 1×10^{-6} m/s	162	16974

[a] Hardware specifications: Intel, 4 core i-5 3.10 GHz, RAM: 16 GB.
[b] Calculation for 5 observation points.
[c] Calculation for 7 observation points (Figure 4 and Figure 5).

robustness. Table 2 provides a summary of the model setups.

For verification plots, temperature changes are observed in time on the *x* direction of the coordinate system (Figure 3).

3.2 *Single BHE*

The Eq. 18 is solved on MATLAB and compared with the numerical results. According to the results, the analytical method solution agrees well with numerical results both under conduction (Figure 4) and advection/dispersion dominated heat transfer systems (Figure 5). Comparing the results of temperature difference between conduction and advection/dispersion heat transfer systems, the impact of the groundwater flow/dispersion appears clearly. The first heat extraction phase generates larger temperature decrease in the point located in the *x*-direction when groundwater flow and dispersion are considered. However, the recovery phase is accelerated due to water flow. Consequently, the subsequent heat extraction induces lower temperature change in the ground close to the BHE. Also, with time, temperature is impacted at larger distance in the direction of the water flow when the groundwater flow and the dispersion are considered (at 10 m, $\Delta T = 0.8$ K with water flow *vs* $\Delta T = 0.2$ K without water flow).

The significant advantage of analytical method can be seen in Table 3. The execution time of Eq. 18 is approximately 1500 times smaller than the runtime of numerical models. Note that, for the analytical solution, the computation time depends on the number of observation point. It has the advantage that it can reduce the calculation time as a function of the amount of required information.

3.3 *Multi-BHEs*

Eq. 20 is solved on MATLAB and compared with the numerical results. According to the results, again the analytical method solution agrees with numerical results both with (Figure 6) and without the groundwater flow (Figure 7).

The small discrepancy between the results of advection/dispersion case can be accounted for the mesh discretization of the numerical simulation. Comparison of Figure 6 and Figure 7 shows that the maximum temperature decrease in the ground is substantially reduced by the groundwater flow (from –12 K to –8 K in the simulated case).

4 SUSTAINABILITY AND RECOVERY ASPECTS

The objective of this section is to evaluate the long-term sustainability of the system and the energy deficit of the ground by comparing the temperature distribution in the vicinity of a BHE and the heat fluxes.

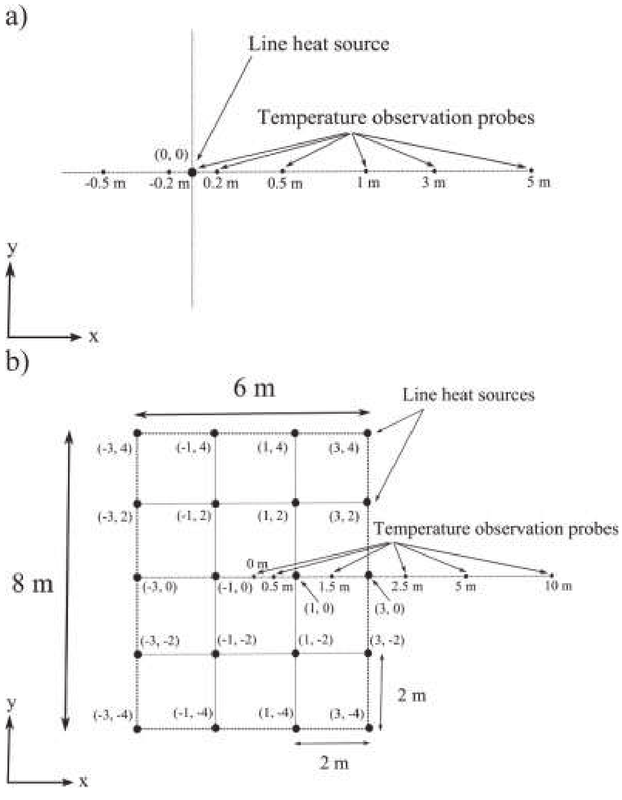

Figure 3. Illustration of temperature observation points on the *x* direction: a) for single BHE b) for multi-BHEs field. Groundwater flow is set on the *x* direction.

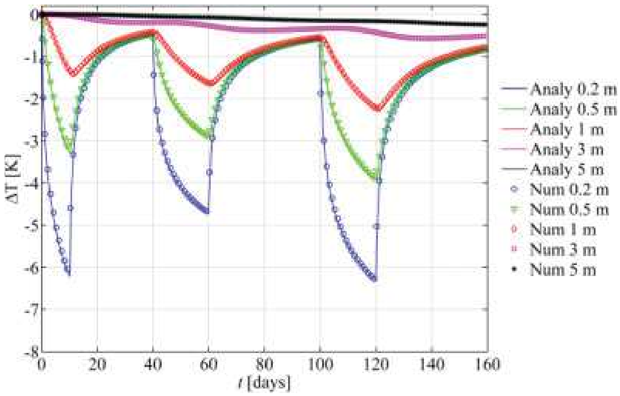

Figure 4. Comparison of numerical and analytical solution results at the depth of 25 m for single line heat source without groundwater flow. Induced by the load profile of Figure 2.

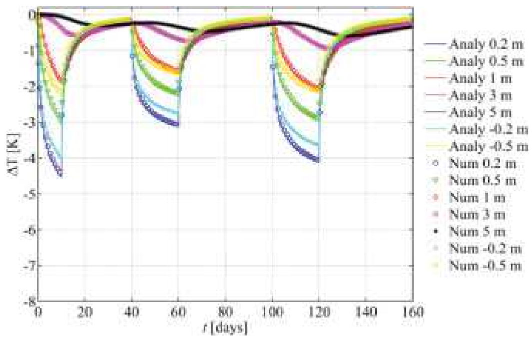

Figure 5. Comparison of numerical and analytical solution results at the depth of 25 m for single line heat source. Under groundwater flow of 1×10^{-6} m/s on the x-axis direction. Induced by the load profile of Figure 2.

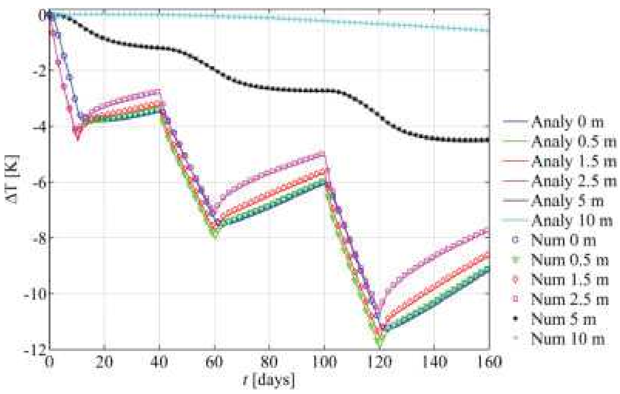

Figure 6. Comparison of numerical and analytical solution results at the depth of 25 m for multi-BHEs field without groundwater flow.

The study is carried out with the developed analytical solution on MATLAB. The scenario contains a production period of 30 years, and a subsequent recovery phase, which is identical duration as the production period. A constant continuous heat extraction of $10.27\,\mathrm{W\,m^{-1}}$ is applied along 30 years operation period (the total amount of heat extraction 9000 kWh per year $= 50\,\mathrm{W\,m^{-1}} \times 100\,\mathrm{m} \times 1800\,\mathrm{h}$ is distributed hourly for a single BHE with a length of 100 m). The bulk thermal conductivity of the ground is $\lambda_m = 1.5\,\mathrm{W\,m^{-1}\,K^{-1}}$, and the bulk volumetric heat

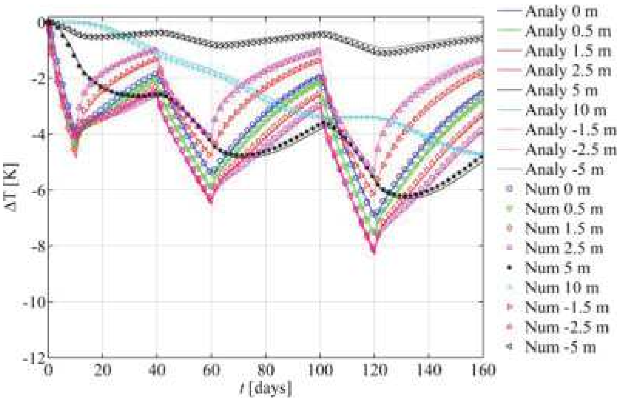

Figure 7. Comparison of numerical and analytical solution results at the depth of 25 m for multi-BHEs field under groundwater flow of 1×10^{-6} m/s on the x-axis direction.

capacity is $2.5\,\mathrm{MJ\,m^{-3}\,K^{-1}}$. The thermal properties of the ground are set as an average value of soils, which can be seen in shallow subsurface such as clay or silica-sand, and the groundwater flow is not considered.

In Figure 8, the relative temperature change results are plotted (e.g. the temperature difference between plume temperature ensuing from the operation and initial ground temperature) during the production and the subsequent recovery phase of the ground. The results show that even at 10 m distance from the BHE, the mean temperature decrease is nearly 0.3 K after 30 years of the ground temperature recovery.

Moreover, the bulk energy deficit of the ground demonstrated in Figure 9 is calculated based on the volume integration method respect to the temperature change. During the production period, the Eq. 20 accounts for the balance between the energy extraction and the lateral heat flux in the ground and during the recovery period only the lateral heat flux in the ground is considered. The bulk energy deficit in the ground can be calculated in axisymmetric conditions as follows:

$$\begin{aligned} Energy &= \int_0^t \int_0^R \int_0^{2\pi} \int_0^H \rho_m c_m \Delta T(z,R,\theta,t)\, dz\,dR\,d\theta\,dt \\ &= 2\pi H \rho_m c_m \int_0^R \sum_{i=0}^{t=60\,years} \Delta T_i(R) R d_R \Delta t \end{aligned} \tag{18}$$

in which H is the length of the BHE and we assume that the energy deficit is identical along the length, ΔT is the temperature change respect to time interval Δt, d_R is the radial distance interval, and R is the radial distance.

Compared to the evaluation of the recovery phase respect to the temperature gradient (Figure 8) and regarding to the energy balance in the ground (Figure 9), it can be seen that the justification based on the local change of the ground temperature does not provide a straight insight compared to the replenishment of the bulk ground energy deficit Actually, the fast decline of the temperature deficit after the shutdown of the system is not translated by such a rapid drop of

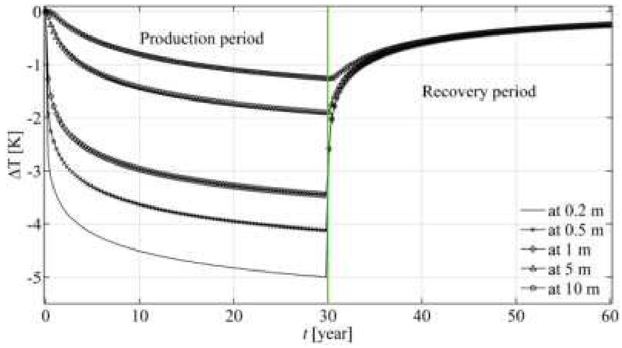

Figure 8. Temperature probe of the scenario. Temperature probes at the depth of 50 m from surface.

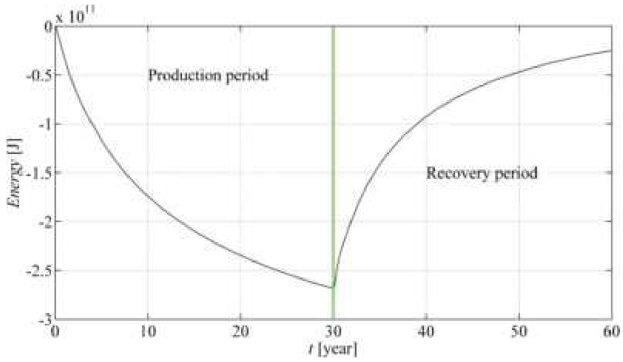

Figure 9. The bulk ground energy deficit of Scenario 4, basalt.

energy deficit. The total amount of extracted energy by the BHE over the production period is around 9.72×10^{11} Joule ($=10.27\,\mathrm{W\,m^{-1}} \times 100\,\mathrm{m} \times 30$ years $\times 3.15 \times 10^7$ s/year) and the net energy deficit in the ground after this 30 years of the production period is around 2.7×10^{11} Joule, which means that approximately 70% of the energy already recovered during the production period by the ground lateral heat fluxes (see Figure 9). After subsequent 30 years of recovery, nearly 98 % of the extracted heat is recovered.

In the near-field, the consideration of the temperature change is plausible to know if the local temperature drops to the freezing point of the groundwater, but the bulk energy deficit gives more global information about the energy recovery of the ground.

5 CONCLUSION

Analytical solutions of GSHP systems are preferable to have a better comprehension about the heat transfer system of the ground. Starting from the Green's function, which is a solution of the conduction/advection/dispersion heat transfer in porous media, we deduced an analytical solution that provides temperature distribution around single and multi-BHEs for intermittent heat extraction or storage. Axial effect and groundwater flow are considered. The proposed analytical solutions are validated with numerical code. Non-symmetric distribution of temperature plume is obtained due to advection and dispersion processes induced by the groundwater movement. The new approach provides significantly shorter computation time compared to numerical simulation to obtain the temperature results of a long-term production of GSHP systems and subsequent recovery period.

The consideration of the temperature change in the vicinity of a BHE does not give the direct insight in the replenishment of the bulk ground energy deficit. By taking into account the bulk vertical and the lateral heat fluxes around the BHEs, the evaluation of the energy recovery may be more realistic.

As a perspective, our analytical model can serve as a tool to predict the ground thermal evaluation around the BHEs during the heat extraction/injection operations and in the subsequent recovery phase after the GSHP system is shutdown. However, the limitations of the model is that we did not take into account the top surface and the bottom heat fluxes which may accelerate the recovery process in long-term, and the performance of the GSHP system may increase more than we estimated here.

ACKNOWLEDGEMENT

The financial support from Walloon Region in Belgium is profoundly acknowledged (Grand: 1117492 – GeoTherWal – Programme ERable (E24+)).

REFERENCES

Bernier, M.A., Labib D.P.R & Pine P. 2004. "A Multiple Load Aggregation Algorithm for Annual Hourly Simulations of GCHP Systems", *HVAC & R Res.* 10 (4): 471–488.

Carslaw, H.S., &. Jaeger J.C. 1959. *Conduction of Heat in Solids, Second Edition*. US-NY: Oxford University Press.

Claesson, J & Eskilson P. 1988. "Conductive Heat Extraction to a Deep Borehole: Thermal Analyses and Dimensioning Rules." *Energy* 13 (6): 509–527.

Deerman, D.J. & Kavanaugh P.S. 1991. "Simulation of Vertical U-Tube Ground – Coupled Heat Pump Systems Using the Cylindrical Heat Source Solution." *ASHRAE Transactions* 97 (1): 287–295.

Diao, N., Li Q., & Fang Z. 2004. "Heat Transfer in Ground Heat Exchangers with Groundwater Advection." *Int. J. of Therm. Sci.* 43 (14): 1203–1211.

Erol S., Hashemi M.A. & François B. (2015). Analytical solution of discontinuous heat extraction for sustainability and recovery aspects of borehole heat exchangers. *Int. J. of Thermal Sciences*, 88, pp. 47–50.

Eskilson, P. 1987. "PhD Thesis: Thermal Analysis of Heat Extraction Boreholes.", Lund: University of Lund.

Gehlin, S. 2002. "PhD. Thesis: Thermal Response Test.", Luleå: Luleå University of Technology.

Hecht-Méndez, J., De Paly M., Beck M. & Bayer P. 2013. "Optimization of Energy Extraction for Vertical Closed-Loop Geothermal Systems Considering Groundwater Flow." *Energy Convers. and Manag.* 66: 1–10.

Hellström, G. 1991. "Ph.D. Thesis: Ground Heat Storage Thermal Analyses of Duct Storage Systems, I. Theory." Lund: University of Lund.

Hopmans, J.W., Šimunek J. & Bristow K.L. 2002. "Indirect Estimation of Soil Thermal Properties and Water Flux

Using Heat Pulse Probe Measurements: Geometry and Dispersion Effects." *Water Resour. Res.* 38 (1): 7–14.

Kavanaugh, S. P., & Rafferty K. 2014. *Geothermal Heating and Cooling: Design of Ground-Source Heat Pump Systems*. *ASHRAE*. Atlanta, US–GA.

Lamarche, L. 2009. "A Fast Algorithm for the Hourly Simulations of Ground-Source Heat Pumps Using Arbitrary Response Factors." *Renew. Energy* 34 (10): 2252–2258.

Man, Y., Yang H., Diao N., Liu J. & Fang Z. 2010. "A New Model and Analytical Solutions for Borehole and Pile Ground Heat Exchangers." *Int. J. Heat Mass Transf.* 53 (13–14): 2593–2601.

Marcotte, D., Pasquier P., Sheriff F., & Bernier M. 2010. "The Importance of Axial Effects for Borehole Design of Geothermal Heat-Pump Systems." *Renew. Energy* 35 (4): 763–770.

Marcotte, D., and Pasquier P. 2008. "Fast Fluid and Ground Temperature Computation for Geothermal Ground-Loop Heat Exchanger Systems." *Geothermics* 37 (6): 651–665.

Metzger, T. 2002. "PhD Thesis (in French): Dispersion Thermique En Milieux Poreux: Caractérisation Expérimentale Par Technique Inverse.", Nancy, Institut national polytechnique de Lorraine (INPL).

Michopoulos, A., & Kyriakis N. 2009. "A New Energy Analysis Tool for Ground Source Heat Pump Systems." *Energy and Buildings* 41 (9): 937–941.

Michopoulos, A., & Kyriakis N. 2010. "The Influence of a Vertical Ground Heat Exchanger Length on the Electricity Consumption of the Heat Pumps." *Renew. Energy* 35 (7): 1403–1407.

Molina-Giraldo, N., Bayer P., & Blum P.. 2011. "Evaluating the Influence of Thermal Dispersion on Temperature Plumes from Geothermal Systems Using Analytical Solutions." *Int. J. of Therm. Sci.* 50 (7): 1223–1231.

Molina-Giraldo, N., Blum P., Zhu K., Bayer P., & Fang Z. 2011. "A Moving Finite Line Source Model to Simulate Borehole Heat Exchangers with Groundwater Advection." *Int. J. of Therm. Sci.* 50 (14): 2506–2513.

Rybach, L., & Eugster W.J.. 2010. "Sustainability Aspects of Geothermal Heat Pump Operation, with Experience from Switzerland." *Geothermics* 39 (4): 365–369.

Sauty, J. P., Gringarten A.C., Fabris H., Thiery D., Menjoz A., & Landel P.A. 1982. "Sensible Energy Storage in Aquifers: 2. Field Experiments and Comparison with Theoretical Results." *Water Resour. Res.* 18 (2): 253–265.

Signorelli, S. 2004. "PhD Thesis: Geoscientific Investigations for the Use of Shallow Low Enthalpy Systems.", Zurich: Swiss Federal Institute of Technology.

Sutton, M. G., Nutter D.W., & Couvillion R.J.. 2003. "A Ground Resistance for Vertical Bore Heat Exchangers With Groundwater Flow." *J. of Energy Resour. Technol.* 125 (3): 183.

VDI-Richtlinie. 2000. "Thermal Use of the Underground – Fundamentals, Approvals and Environmental Aspects, VDI 4640 Blatt 1." Düsseldorf: Verain Deutscher Ingenieure, VDI-Verlag.

Yavuzturk, C. 1999. "PhD Thesis: Modeling of Vertical Ground Loop Heat Exchangers for Ground Source Heat Pump Sytems." US-OK: Oklahoma State University.

Zeng, H. Y., N.R. Diao, & Fang Z.H.. 2002. "A Finite Line-Source Model for Boreholes in Geothermal Heat Exchangers." *Heat Transfer Asian Research* 31 (7): 558–567.